Eur Radiol (2015) 25:2701–2708
DOI 10.1007/s00330-015-3659-6

NUCLEAR MEDICINE

Quantification of tumour ^{18}F-FDG uptake: Normalise to blood glucose or scale to liver uptake?

Georgia Keramida · Sabina Dizdarevic · Janice Bush · A. Michael Peters

Received: 3 September 2014 / Revised: 7 January 2015 / Accepted: 4 February 2015 / Published online: 22 April 2015

Abstract
Purpose To compare normalisation to blood glucose (BG) with scaling to hepatic uptake for quantification of tumour ^{18}F-FDG uptake using the brain as a surrogate for tumours.
Methods Standardised uptake value (SUV) was measured over the liver, cerebellum, basal ganglia, and frontal cortex in 304 patients undergoing ^{18}F-FDG PET/CT. The relationship between brain FDG clearance and SUV was theoretically defined.
Results Brain SUV decreased exponentially with BG, with similar constants between cerebellum, basal ganglia, and frontal cortex (0.099–0.119 mmol/l^{-1}) and similar to values for tumours estimated from the literature. Liver SUV, however, correlated positively with BG. Brain-to-liver SUV ratio therefore showed an inverse correlation with BG, well-fitted with a hyperbolic function (R=0.83), as theoretically predicted. Brain SUV normalised to BG (nSUV) displayed a nonlinear correlation with BG (R=0.55); however, as theoretically predicted, brain nSUV/liver SUV showed almost no correlation with BG. Correction of brain SUV using BG raised to an exponential power of 0.099 mmol/l^{-1} also eliminated the correlation between brain SUV and BG.
Conclusion Brain SUV continues to correlate with BG after normalisation to BG. Likewise, liver SUV is unsuitable as a reference for tumour FDG uptake. Brain SUV divided by liver SUV, however, shows minimal dependence on BG.
Key Points
- *FDG standard uptake value in tumours helps clinicians assess response to treatment.*
- *SUV is influenced by blood glucose; normalisation to blood glucose is recommended.*
- *An alternative approach is to scale tumour SUV to liver SUV.*
- *The brain used as a tumour surrogate shows that neither approach is valid.*
- *Applying both approaches, however, appropriately corrects for blood glucose.*

Keywords FDG · Tumour SUV · Liver SUV · Brain SUV · Hepatic steatosis

G. Keramida · S. Dizdarevic · J. Bush · A. M. Peters
Clinical Imaging Sciences Centre, Brighton and Sussex Medical School, Brighton, UK

G. Keramida · S. Dizdarevic · A. M. Peters
Department of Nuclear Medicine, Brighton and Sussex University Hospitals NHS Trust, Brighton, UK

G. Keramida (✉)
Clinical Imaging Sciences Centre, University of Sussex, Falmer, Brighton BN1 9RR, UK
e-mail: G.Keramida@bsms.ac.uk

Introduction

In the use of 2-deoxy-2-fluoro-D-glucose ^{18}F-FDG positron emission tomography–computed tomography (PET/CT) for cancer management, some form of quantification of tumour uptake is essential in order to monitor treatment. This is most often done by measuring the standardised uptake value (SUV), which is the fraction of administered activity per millilitre of tissue, multiplied by an index of body size, usually weight. An alternative approach is to scale tumour count to the count rate from the liver, which in this context is assumed to be relatively constant. Because tumour SUV is inversely related to blood glucose, European Association of Nuclear Medicine (EANM) guidelines recommend normalisation of tumour SUV to blood glucose of 5 mmol/l [1]. This approach assumes a tumour glucose utilisation rate (MR_{GLU}) that is

independent of blood glucose, in which MR_{GLU} would be equal to the product of tumour FDG clearance (ignoring the lumped constant [LC]) and blood glucose. Thus, insofar as tumour SUV is a surrogate for tumour FDG clearance, the guidelines assume a hyperbolic relationship between tumour SUV and blood glucose. EANM guidelines also recommend rescheduling the study if blood glucose is above 7 mmol/l, although most departments would tolerate levels up to 10 mmol/l.

Liver SUV (SUV_{liver}) is thought to be relatively constant [2, 3] and so an alternative approach is to express tumour count rate as a ratio with liver count rate [4–7]. The validity of this approach has received recent attention given the potential effect of hepatic steatosis on liver FDG uptake. Several groups have examined the relationship between steatosis and SUV_{liver}. The results, however, were conflicting [8–12], likely because the effects of blood glucose on hepatic SUV were ignored.

FDG is dynamically exchanged between hepatocytes and blood (Fig. 1), resulting in a hepatic FDG concentration that closely mirrors the blood concentration [13–16]. Indeed, it has been recommended that in small animal work, the liver is a better region than the heart for monitoring the time course of blood activity [15]. Because blood FDG concentration is dependent on blood glucose [13], the hepatic FDG signal, rather than being constant, is also dependent on blood glucose, as has been previously shown [17, 18], such that the tumour-to-liver ratio also depends on blood glucose.

The aim of this study was to compare the normalisation to blood glucose and scaling to the liver as correction procedures for quantification of tumour FDG uptake. Tumour SUV is highly variable in patients with cancer, so we used the brain as a surrogate for tumours to examine the effects of blood glucose. The justification for this relies on the premise that FDG uptake kinetics should be similar for tissues such as brain and tumour, but unlike liver, in which FDG is metabolically trapped.

In order to evaluate the impact of hepatic steatosis on scaling to the liver, we also compared the relationship between brain-to-liver SUV ratio and blood glucose in patients with and without hepatic steatosis. Finally, we explored an additional procedure that may be useful for correcting tumour FDG uptake for blood glucose.

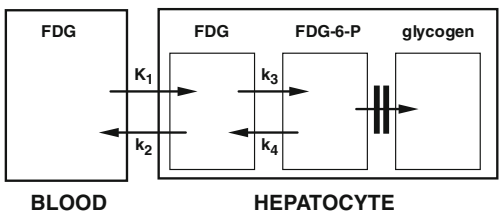

Fig. 1 Model depicting the kinetics of FDG between blood and hepatocyte. FDG is phosphorylated in the hepatocyte (k_3) but is not incorporated into glycogen. Following dephosphorylation (k_4), it diffuses back into blood (k_2). K_1 represents hepatic blood flow

Methods

Patients

This was a retrospective service evaluation based on 304 patients undergoing routine FDG PET/CT. We initially included a consecutive group of 156 patients over a two-year period (2011–2012). To increase the numbers of patients with low or high blood glucose levels, we included 148 additional patients with blood glucose levels>6 (n =113) or<4 (n=35) mmol/l who underwent imaging between 2007 and 2012. Most patients were referred with cancer. Forty-seven patients were currently receiving chemotherapy and 56 had received chemotherapy previously.

All patients who visit our PET CT unit are asked to provide informed consent for use of any of their clinical data for publication, and all patients in this study did so.

PET/CT acquisition

Departmental protocol dictated that patients fast for at least 6 hours prior to their appointment. Blood glucose was measured using a glucometer (Accu-Chek Performa, Accu-Chek Inform II test strips; Roche Diagnostics, Indianapolis, IN, USA). FDG was injected intravenously via the antecubital fossa or hand. Patients were required to relax in a semi-recumbent position in a warm, quiet area during the uptake period. Imaging was performed 60 min post-injection of 400 MBq (±10 %) FDG.

A Siemens Biograph 64-slice PET with immediate non-enhanced CT imaging (120 kVp/50 mA—CARE Dose 4D; slice, 5 mm; pitch, 0.8; rotational speed, 0.5/sec), was used to cover the area from the orbital margin to the lesser trochanters. Arms were up, as arms down may result in artificial elevation of the liver FDG signal due to beam-hardening effects. Three-dimensional emission data were then acquired at 3 min per bed position (PET reconstruction: 4 iterations; subset, 8; Gaussian pre-filter; full width at half maximum (FWHM), 5 mm; matrix size, 168×168; zoom, 1).

Image analysis

Regions of interest (ROIs) were drawn over the right lobe of the liver (3 cm diameter, avoiding any focal lesions), frontal cortex (1.5 cm), basal ganglia (0.9 cm), and cerebellum (1.6 cm). The whole-body sweep did not include frontal cortex and basal ganglia in 107 patients. Maximum and average standardised uptake values (SUV_{max} and SUV_{ave}) were recorded for all four regions. An ROI identical to the liver

ROI drawn on the PET image was drawn on the CT scan for measurement of CT density in Hounsfield units (HU). SUV in brain regions was multiplied by blood glucose and divided by 5 to give normalised SUV (nSUV).

Statistical analysis

The relationships between variables were quantified using Pearson's linear regression analysis of continuous data. In addition, patients were categorised into six subgroups based on blood glucose within the following ranges (patient numbers in brackets): < 4 (59), 4–4.9 (76), 5–5.9 (38), 6–7.9 (38), 8–9.9 (58), and 10+ (35) mmol/l. Patients were also subdivided into those with hepatic steatosis (CT density<40 HU; n=71) and those without (>39 HU; n=233) [19, 20].

Results

Relationship between blood glucose and hepatic CT density

There was an inverse relationship between blood glucose and hepatic CT density (R=−0.39, p<0.0001; Fig. 2). Thus, patients with fatty liver tend to have high blood glucose.

Relationships of brain and hepatic SUV values with blood glucose

Cerebellar SUV_{max} declined non-linearly as a function of blood glucose (Fig. 3). The relationship was better fitted with an exponential function, the constant of which was −0.0993 mmol/l^{-1} (R=0.75), than a hyperbolic function (R=0.60). Corresponding exponential constants for frontal cortex and basal ganglia SUV_{max} were −0.119 mmol/l^{-1} (R=0.76) and −0.114 mmol/l^{-1} (R=0.75). Exponential constants for brain SUV_{ave} were similar: −0.113 (R=0.77), −0.110 (R=0.76), and −0.097 (R=0.74) mmol/l^{-1} for the frontal cortex, basal ganglia, and cerebellum, respectively. In contrast, liver SUV increased non-linearly as blood glucose increased (Fig. 4).

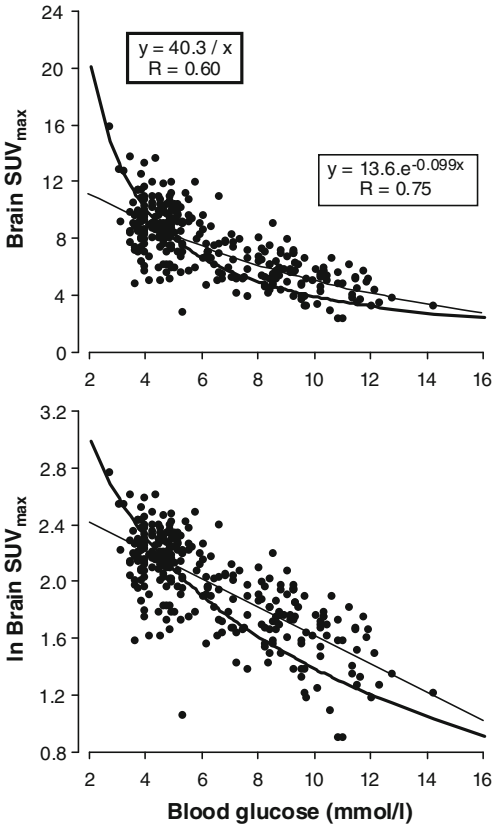

Fig. 3 Relationship between cerebellar SUV_{max} and blood glucose. Equations are shown for least squares fits to hyperbolic (y=K/x; *bold line*) and exponential (*fine line*) functions. *Upper panel:* linear ordinate; *lower panel*: logarithmic ordinate

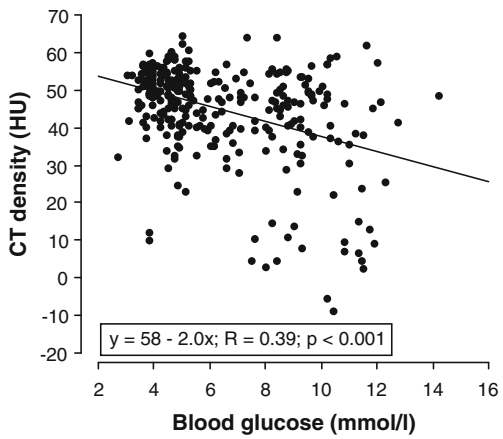

Fig. 2 Relationship between liver CT density (HU) and blood glucose. *Straight line* is linear fit

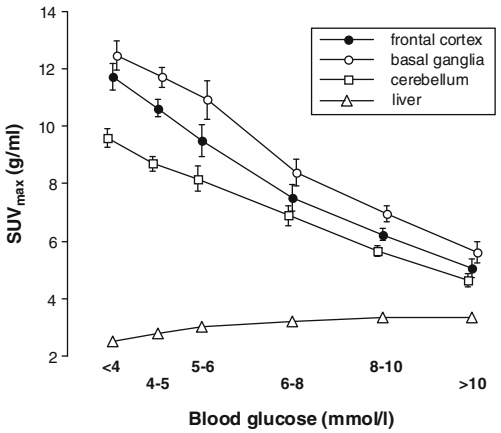

Fig. 4 Relationships of brain SUV_{max} to liver SUV_{max} ratio with blood glucose. *Vertical bars*=SEM. Note that SEM values for the liver are too small to be visible

Relationship between cerebellum-to-liver SUV ratio and blood glucose

The ratio of cerebellum-to-liver SUV_{max} declined non-linearly as blood glucose increased (Fig. 5). The relationship appeared hyperbolic (R=0.83), as theoretically predicted (see Appendix; Eq. 12). The relationship between cerebellum SUV_{max}/liver SUV_{ave} and blood glucose was similar (data not shown).

Effect of hepatic steatosis on the relationship between cerebellum/liver SUV ratio and blood glucose

The relationships between cerebellum-to-liver SUV ratios and blood glucose were similar patients with and without hepatic steatosis, whether SUV_{max} or SUV_{ave} was the denominator (Fig. 6).

Correction of brain SUV for blood glucose

Correction of tumour SUV for blood glucose by normalisation to 5 mmol/l (nSUV) aims to abolish the dependence of tumour SUV on blood glucose, and the same should apply to the brain. However, normalisation gave $nSUV_{max}$ values for the cerebellum that correlated in a complex manner with blood glucose (Fig. 7a, *upper panel*). Thus, there was a positive correlation up to blood glucose level of 7 mmol/l, with a gradient of ~1 SUV per mmol/l (R=0.44; p<0.0001), but no further increase above 7 mmol/l. The overall relationship was therefore better fitted with a second-order polynomial (R=0.55).

Division of cerebellar $nSUV_{max}$ by liver SUV_{max} almost abolished its relationship with blood glucose, leaving a small gradient of 0.04 SUV per mmol/l (R=0.17; p<0.01; Fig. 7b, *upper panel*). There was no difference in this relationship between patients with and without hepatic steatosis. Results were similar when cerebellar $nSUV_{max}$ was divided by liver SUV_{ave}

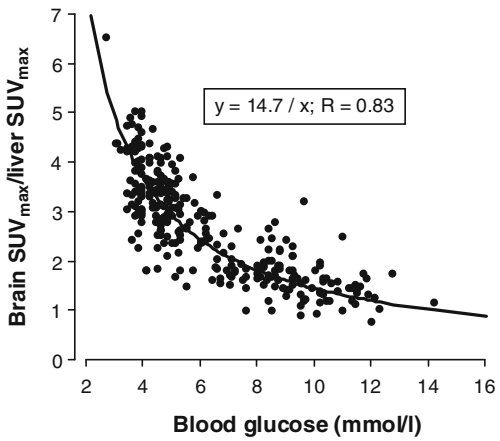

Fig. 5 Relationship between brain SUV_{max} (cerebellum) to liver SUV_{max} ratio (y) and blood glucose (x): y=14.7/x

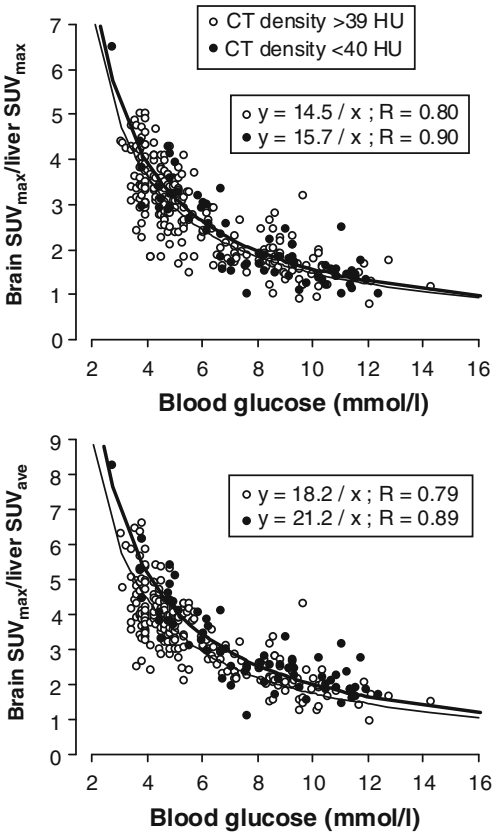

Fig. 6 Relationships of brain SUV_{max} (cerebellum) to liver SUV ratios with blood glucose in patients with (*closed circles, bold line*) and without (*open circles, faint line*) hepatic steatosis. *Upper panel*: cerebellar SUV_{max}/liver SUV_{max}; *lower panel*: cerebellar SUV_{max}/liver SUV_{ave}. Least square fits to hyperbolic functions are shown. In both panels, the fits to steatosis and non-steatosis patients are similar

instead of SUV_{max}, although the correlation coefficient and regression gradient were slightly higher (Fig. 7b, *lower panel*).

Based on the exponential constant of −0.099 $mmol/l^{-1}$ derived from the relationship between cerebellum SUV_{max} and blood glucose, multiplication of basal ganglia SUV_{ave} with $e^{0.099.glucose}$ gave corrected SUV values that showed no correlation with blood glucose (R=0.03; Fig. 7a, *lower panel*). Application of this correction procedure to the frontal cortex yielded similar results (data not shown).

Discussion

Brain SUV as a function of blood glucose

FDG enters the cell using the same transport system and phosphorylation enzymes as glucose, but is then metabolically trapped. As Hasselbalch et al. [21] found no change in regional cerebral MR_{GLU} in response to acute hyperglycaemia, elevated blood glucose levels should result in decreased FDG uptake in the brain. Accordingly, we found an inverse nonlinear relationship between brain SUV and blood glucose that was well fitted

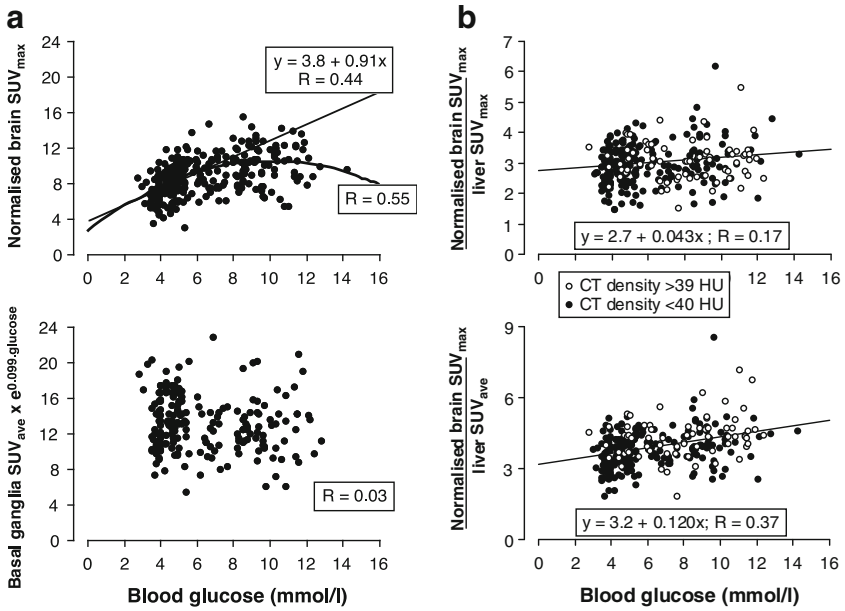

Fig. 7 **a** Relationships with blood glucose of brain SUV normalised to blood glucose. *Upper panel*: cerebellar SUV_{max} normalised to blood glucose of 5 mmol/l. *Straight line* is linear fit to points up to blood glucose of 7 mmol/l. *Bold curved line* is second-order polynomial fit to all data. *Lower panel*: basal ganglia SUV_{ave} corrected for blood glucose by multiplication with $e^{0.099 \times glucose}$, where the exponential constant of 0.099 mmol/l was derived from the exponential relationship between SUV_{max} of the cerebellum and blood glucose (*see* Fig. 3). Correlation coefficients (*R*) are shown in each panel. **b** Relationships with blood glucose of brain SUV normalised to blood glucose (nSUV) and then divided by liver SUV. *Upper panel*: cerebellar $nSUV_{max}$ divided by liver SUV_{max}; *lower panel*: cerebellar $nSUV_{max}$ divided by liver SUV_{ave}. Patients with hepatic steatosis (HU<40) are shown as *open circles* and those without (HU>39) as *closed circles. Straight lines* are linear fits to all data points

by an exponential function. An inverse relationship between brain SUV and blood glucose has been shown previously in works by others [22, 23]. Buchert et al. [24] showed that acute reversal of hyperglycaemia increased FDG uptake in the brain by up to 80 %, while Kawasaki et al. [25] found that mild hyperglycaemia affected the distribution of FDG uptake in the brain of normal subjects. Critically, exponential constants of the relationships between brain SUV and blood glucose in the current study were similar for the cerebellum, basal ganglia, and frontal cortex.

Validity of liver SUV for scaling tumour SUV: effects of steatosis and blood glucose

Liver SUV, in contrast to brain SUV, showed a positive relationship with blood glucose (Fig. 4). The brain/liver SUV ratio, therefore, showed a strong inverse relationship with blood glucose (Fig. 5). As theoretically predicted (Appendix), this was hyperbolic. Although much attention has recently been focussed on the influence of hepatic steatosis on the validity of liver SUV as a comparator for tumour FDG uptake [8–12], blood glucose clearly has a more dramatic effect than hepatic fat on the brain-to-liver SUV ratio. Recent studies addressing the validity of the fatty liver as a comparator did not consider the influence of blood glucose on hepatic SUV, even though patients with fatty liver disease tend to have high blood glucose, as shown in Fig. 2. Two recent studies from our group [26, 27] confirmed that when blood glucose is taken into account, FDG accumulation in the liver is increased in hepatic steatosis. However, as shown in the current study, steatosis has much less impact on scaling brain SUV to liver SUV in comparison to blood glucose.

Use of brain SUV as a surrogate for tumour FDG uptake

Hasselbalch et al. [21] measured MR_{GLU} in the brains of normal subjects using the Sokoloff model. The authors showed that during acute hyperglycaemia in comparison to normoglycaemia, there was no change in global or regional MR_{GLU} in cortical and subcortical grey matter. Most studies [23, 28–30], though not all [31, 32], have shown that tumour SUV also decreases at high blood glucose levels, as is recognised in both the EANM and the Society of Nuclear Medicine guidelines [1, 33]. Lindholm et al. [28] showed no change in tumour MR_{GLU} in response to oral glucose loading in five patients with head and neck cancer. Moreover, Crippa et al. [29] recorded a decrease in mean SUV of 20 hepatic colorectal metastatic deposits from 9.4 to 4.3 in a study in which patients underwent imaging on two separate occasions: fasting, and following a glucose load that increased blood glucose from 5 to 9 mmol/l. Ishizu et al. [23] recorded a decrease in brain glioma SUV from 4.41 to 1.54 associated

with an increase in blood glucose from 5.9 to 13.5 mmol/l. Insofar as the brain can be regarded as a surrogate for tumours, in that both display no change in MR_{GLU} in relation to glucose levels, the liver clearly cannot be used as a tissue comparator for tumour FDG uptake.

Correction of tumour SUV for blood glucose

The similarity between brain and tumour FDG kinetics can be extended to the correction of tumour SUV for blood glucose. EANM guidelines recommend normalising tumour SUV to 5 mmol/l [1]. To be successful, this procedure is required to abolish any relationship between tumour SUV and blood glucose. Its validity in this respect is supported by some studies [34, 35] but not by others [31].

A critical assumption underlying the use of the brain as a surrogate for tumour FDG uptake is that MR_{GLU} in the brain and tumours is independent of blood glucose. There is little robust *quantitative* data in the literature concerning the effects of blood glucose on tumour SUV. Assuming an inverse exponential relationship between tumour SUV and blood glucose, it can be calculated from the data of Lindholm et al. [28] that the exponential constant for tumours would be −0.1 to −0.15 $mmol/l^{-1}$. Based on the data of Crippa et al. [29], the constant would be about−0.2 $mmol/l^{-1}$, although their SUV values had very high standard deviations. Based on the data of Ishizu et al. [23], the constant would be −0.093 mmol/l. These estimated exponential constants are broadly similar to those recorded here for the brain (−0.099 to −0.119 $mmol/l^{-1}$).

Given the variation in tumour SUV, it is difficult to determine the relationship between blood glucose and tumour SUV in large heterogeneous patient populations. Nevertheless, in such an attempt, Zhuang et al. [30] recorded a weak inverse correlation between tumour SUV and blood glucose, without indicating whether the relationship was hyperbolic, exponential, or linear. In contrast, in 248 patients with lung cancer, Hallet et al. [31] found no significant correlation between tumour SUV, *expressed logarithmically* (thereby implying an exponential relation), and blood glucose. Differing levels of metabolic activity across tumours would not rule out a unique exponential constant that could be universally applied to tumours, provided that tumour MR_{GLU}, like brain MR_{GLU}, is independent of blood glucose.

In the current study, normalisation failed to achieve independence of the brain nSUV in relation to blood glucose, and instead generated a significant nonlinear correlation (Fig. 7). However, when brain $nSUV_{max}$ was divided by liver SUV_{max}, it showed almost no relationship with blood glucose, regardless of whether patients had hepatic steatosis (Fig. 7). This finding is consistent with Eq. 12 (Appendix), which shows that (tissue SUV [SUVi]×blood glucose)/SUV_{liver} is constant. When brain $nSUV_{max}$ was divided by liver SUV_{ave} instead of SUV_{max}, a moderate linear positive correlation remained with blood glucose. We believe this is the result of a 'signal dilution' effect on liver SUV_{ave} of excess hepatic fat, the distribution of which is not homogeneous [36]. Such a dilutive effect is less with SUV_{max} than SUV_{ave} because SUV_{max} is selectively based on a voxel that is relatively free of fat [26]. The correlation between brain $nSUV_{max}$/liver SUV_{ave} and glucose is then the result of higher levels of hepatic fat in patients with high blood glucose. As such, for this dual correction procedure, liver SUV_{max} is recommended. The sense of the procedure is evident when, for example, there is heavy uptake of FDG by bone marrow. This would reduce the availability of FDG uptake elsewhere and reduce left ventricular blood SUV (SUV_{LV}) and SUV_{liver}. Division of nSUV by SUV_{liver} would then appropriately increase nSUV. Another attractive feature of this approach is that it avoids the emerging issue of the best whole-body index—weight, lean body mass, or body surface area—upon which to base SUV [37], since whatever index used for measuring SUV is cancelled out.

Multiplication of SUV by $e^{0.099 \times glucose}$ (based on the exponential constant of 0.099 $mmol/l^{-1}$ for the relationship between cerebellar SUV_{max} and blood glucose) is another potential correction procedure. It abolishes the relationship between basal ganglia SUV and blood glucose (Fig. 7a). If a constant of approximately −0.1 $mmol/l^{-1}$ is not universal for tumours, this correction would then not be valid for tumours. Further work is needed to address this issue, particularly in regard to the independence of tumour MR_{GLU} and blood glucose level.

Study limitations

Limitations of the study include its retrospective design and heterogeneous patient population. Whilst every effort was made to avoid any focal liver pathology when drawing the liver ROI, it is possible that covert pathology, such as diffuse colorectal micrometastases, may have increased liver SUV. Moreover, the frontal cortex and basal ganglia were included in the whole-body sweep in only two-thirds of the patients, although patient numbers were still high.

Conclusions

In conclusion, tumour FDG uptake cannot be factored to liver SUV because of the effects of blood glucose rather than any influence of hepatic fat. Normalisation of brain SUV to blood glucose results in a complex relationship with blood glucose and is therefore also invalid. Combining the two correction procedures, however, gives corrected values that show almost no relationship with blood glucose, and the success of this dual correction procedure is explained theoretically in the Appendix. Normalisation to blood glucose using an exponential constant could also be useful.

Acknowledgments The scientific guarantor of this publication is Michael Peters. The authors of this manuscript declare no relationships with any companies whose products or services may be related to the subject matter of the article. The authors state that this work has not received any funding. No complex statistical methods were necessary for this paper. Institutional Review Board approval was obtained. Written informed consent was obtained from all subjects (patients) in this study. Some study subjects or cohorts have been previously reported in AJR 2014;203:643–8 and Eur J Radiol 2014;83:751–5. Methodology: retrospective, observational, performed at one institution.

Appendix

The EANM guidelines recommend normalisation of tumour SUV to blood glucose of 5 mmol/l. This presupposes a hyperbolic relationship (i.e., y=constant/x) between SUV and blood glucose.

MR_{GLU} in tissues in which FDG is metabolically trapped is related to tissue FDG clearance rate (Zi) and blood glucose concentration (G), as follows [21]:

$$MR_{GLU} = Zi \times G \times LC \quad (1)$$

Where LC is lumped constant.

Rearranging Eq. 1 and ignoring LC,

$$Zi = MR_{GLU}/G \quad (2)$$

Assuming MR_{GLU} is constant, this indicates a hyperbolic relationship between Zi and G.

Tissue SUV (SUVi) is a surrogate for Zi but is not identical to it. It is related to Zi as follows.

$$Zi = M(t)/area(t), \quad (3)$$

where M(t) and area(t) are respectively the quantity of FDG accumulated in the tissue and the area under the blood FDG time-concentration curve at time t (60 min in the current study).

Substituting for Zi in Eq. 1

$$MR_{GLU} = M(t)/area(t) \times G \quad (4)$$

$$\text{Now } SUVi = M(t)/V \; x \; W/M(0), \quad (5)$$

where V is tissue volume, W is body weight and M(0) is administered activity.

Rearranging Eq. 5

$$M(t) = SUVi \text{ x } V/W \text{ x } M(0) \quad (6)$$

Substituting for M(t) in Eq. 4 and rearranging,

$$MR_{GLU}/V = SUVi \text{ x } M(0)/W \times G/area(t) \quad (7)$$

For typical FDG blood clearance half-times of around 50 min from completion of early mixing (~10 min) [20], area(60 min) is approximately proportional to C(60 min), where C(t) is the blood concentration of FDG. For example, comparing clearance half-times of 69 and 50 min, the concentration and area ratios are 1.28 and 1.11, respectively, similar to the corresponding ratios for half-times of 50 and 39 min (1.26 and 1.11); i.e., same error.

So, substituting C(t) for area(t) in Eq. 7 and ignoring the proportionality constant,

$$MR_{GLU}/V = SUVi \times M(0)/W \times G/C(t) \quad (8)$$

Analogous to Eq. 5,

$$\text{left ventricular blood SUV } (SUV_{LV}) = C(t) \times W/M(0) \quad (9)$$

Substituting for C(t) in Eq. 8,

$$MR_{GLU}/V = SUVi/SUV_{LV} \times G \quad (10)$$

Rearranging Eq. 10,

$$SUVi/SUV_{LV} = MR_{GLU}/V \times 1/G \quad (11)$$

So $SUVi/SUV_{LV}$, rather than SUVi, has a hyperbolic relationship with blood glucose and therefore more closely represents Zi. Because of the kinetics of FDG distribution between hepatocytes and blood, liver FDG concentration closely reflects blood FDG concentration [13–16]. In Eq. 11, therefore, SUV_{LV} can be replaced by SUV_{liver}:

$$SUVi/SUV_{liver} = MR_{GLU}/V \times 1/G \quad (12)$$

Alternatively, the relationship between SUVi and blood glucose can be regarded as exponential, i.e.,

$$SUVi = A.e^{-k.G} \quad (13)$$

The exponential constant k is the fractional decrease in SUVi per unit increase in blood glucose, and intuitively should be constant for tissues that metabolically trap FDG. Tissue MR_{GLU} would then be reflected by A.

References

1. Boellaard R, O'Doherty MJ, Weber WA, Mottaghy FM, Lonsdale MN, Stroobants SG et al (2010) FDG PET and PET/CT: EANM procedure guidelines for tumour PET imaging: version 1.0. Eur J Nucl Med Mol Imaging 37:181–200
2. Paquet N, Albert A, Foidert J, Hustinx R (2004) Within-patient variability of ^{18}F-FDG: standardized uptake values in normal tissues. J Nucl Med 45:784–788
3. Ramos CD, Erdi YE, Gonen M, Riedel E, Yeung HW, Macapinlac HA et al (2001) FDG-PET standardized uptake values in normal anatomic structures using iterative reconstructed segmented attenuation correction and filtered back-projection. Eur J Nucl Med 28:155–164
4. Khandani AH, Wahl RL (2005) Applications of PET in liver imaging. Radiol Clin N Am 43:849–860
5. Kumar R, Xiu Y, Yu JQ, Takalkar A, El-Haddad G, Potenta S et al (2004) ^{18}F-FDG PET in evaluation of adrenal lesions in patients with lung cancer. J Nucl Med 45:2058–2062
6. van Kouwen MC, Jansen JB, van Goor H, de Castro S, Oyen WJ, Drenth JP (2005) FDG-PET is able to detect pancreatic carcinoma in chronic pancreatitis. Eur J Nucl Med Mol Imaging 32:399–404
7. Diederichs CG, Staib L, Glatting G, Beger HG, Reske SN (1998) FDG PET: Elevated plasma glucose reduces both uptake and detection rate of pancreatic malignancies. J Nucl Med 39:1030–1033
8. Bural GG, Torigian DA, Burke A, Houseni M, Alkhawaldeh K, Cucchiara A et al (2010) Quantitative assessment of the hepatic metabolic volume product in patients with diffuse hepatic steatosis and normal controls through use of FDG-PET and MR imaging: a novel concept. Mol Imaging Biol 12:233–239
9. Abikhzer G, Alabed YZ, Azoulay L, Assayag J, Rush C (2011) Altered hepatic metabolic activity in patients with hepatic steatosis on FDGPET/CT. AJR Am J Roentgenol 196:176–180
10. Lin CY, Lin WY, Lin CC, Shih CM, Jeng LB, Kao CH (2011) The negative impact of fatty liver on maximum standard uptake value of liver on FDG PET. Clin Imaging 35:437–441
11. Abele JT, Fung CI (2010) Effect of hepatic steatosis on liver FDG uptake measured in mean standard uptake values. Radiology 254: 917–924
12. Kamimura K, Nagamachi S, Wakamatsu H, Higashi R, Ogita M, Ueno S et al (2010) Associations between liver (18)F fluoro-2-deoxy-D-glucose accumulation and various clinical parameters in a Japanese population: influence of the metabolic syndrome. Ann Nucl Med 24:157–161
13. Choi Y, Hawkins RA, Huang SC, Brunken RC, Hoh CK, Messa C et al (1994) Evaluation of the effect of glucose ingestion and kinetic model configurations of FDG in the normal liver. J Nucl Med 35: 818–823
14. Oya N, Nagata Y, Ishigaki T, Abe M, Tamaki N, Magata Y et al (1993) Evaluation of experimental liver tumors using fluorine- 18-2-fluoro-2-deoxy-d-glucose PET. J Nucl Med 34:2124–2129
15. Green LA, Gambhir SS, Srinivasan A, Banerjee PK, Hoh CK, Cherry SR et al (1998) Noninvasive methods for quantitating blood time-activity curves from mouse pet images obtained with fluorine-18-fluorodeoxyglucose. J Nucl Med 39:729–734
16. Torizuka T, Tamaki N, Inokuma T, Magata Y, Sasayama S, Yonekura Y et al (1995) In vivo assessment of glucose metabolism in hepatocellular carcinoma with FDG PET. J Nucl Med 36:1811–1817
17. Kubota K, Watanabe H, Murata Y, Yukihiro M, Ito K, Morooka M et al (2011) Effects of blood glucose level on FDG uptake by liver: a FDG-PET/CT study. Nucl Med Biol 38:347–351
18. Groheux D, Delord M, Rubello D, Colletti PM, Nguyen M-L, Hindie E (2013) Variation of liver SUV on ^{18}FDG-PET/CT studies in women with breast cancer. Clin Nucl Med 38:422–425
19. Boyce CJ, Pickhardt PJ, Kim DH, Taylor AJ, Winter TC, Bruce RJ et al (2010) Hepatic steatosis (fatty liver disease) in asymptomatic adults identified by unenhanced low-dose CT. AJR Am J Roentgenol 194:623–628
20. Zeb I, Li D, Nasir K, Katz R, Larijani VN, Budoff MJ (2012) Computed tomography scans in the evaluation of fatty liver disease in a population based study: the multi-ethnic study of atherosclerosis. Acad Radiol 19:811–818
21. Hasselbalch SG, Knudsen GM, Capaldo B, Postiglione A, Paulson OB (2001) Blood–brain barrier transport and brain metabolism of glucose during acute hyperglycemia in humans. J Clin Endocrinol Metab 86:1986–1990
22. Claeys J, Mertens K, D'Asseler Y, Goethals I (2010) Normoglycemic plasma glucose levels affect F-18 FDG uptake in the brain. Ann Nucl Med 24:501–505
23. Ishizu K, Nishizawa S, Yonekura Y, Sadato N, Magata Y, Tamaki N et al (1994) Effects of hyperglycemia on FDG uptake in human brain and glioma. J Nucl Med 35:1104–1109
24. Buchert R, Santer R, Brenner W, Apostolova I, Mester J, Clausen M et al (2009) Computer simulations suggest that acute correction of hyperglycaemia with an insulin bolus protocol might be useful in brain FDG PET. Nuklearmedizin 48:44–54
25. Kawasaki K, Ishii K, Saito Y, Oda K, Kimura Y, Ishiwata K (2008) Influence of mild hyperglycemia on cerebral FDG distribution patterns calculated by statistical parametric mapping. Ann Nucl Med 22: 191–200
26. Keramida G, Potts J, Bush J, Dizdarevic S, Peters AM (2014) Hepatic steatosis is associated with increased hepatic FDG uptake. Eur J Radiol 83:751–755
27. Keramida G, Potts J, Bush J, Verma S, Dizdarevic S, Peters AM (2014) Accumulation of ^{18}F-FDG in the Liver in Hepatic Steatosis. Am J Roentgenol 203:643–648
28. Lindholm P, Minn H, Leskinen-Kallio S, Bergman J, Ulla Ruotsalainen U, Heikki Joensuu H (1993) Influence of the blood glucose concentration on FDG uptake in cancer - a PET study. J Nucl Med 34:1–6
29. Crippa F, Gavazzi C, Bozzetti F, Chiesa C, Pascali C, Bogni A et al (1997) The influence of blood glucose levels on [^{18}F]fluorodeoxyglucose (FDG) uptake in cancer: a PET study in liver metastases from colorectal carcinomas. Tumori 83:748–752
30. Zhuang HM, Cortes-Blanco A, Pourdehnad M, Adam LE, Yamamoto AJ, Martinez-Lazaro R et al (2001) Do high glucose levels have differential effect on FDG uptake in inflammatory and malignant disorders? Nucl Med Commun 22:1123–1128
31. Hallett WA, Marsden PK, Cronin BF, O'Doherty MJ (2001) Effect of corrections for blood glucose and body size on [^{18}F]FDG PET standardised uptake values in lung cancer. Eur J Nucl Med 28:919–922
32. Busing KA, Schonberg SO, Brade J, Wasser K (2013) Impact of blood glucose, diabetes, insulin, and obesity on standardized uptake values in tumors and healthy tissues. Nucl Med Biol 40:206–213
33. Delbeke D, Coleman RE, Guiberteau MJ, Brown ML, Royal HD, Siegel BA et al (2006) Procedure guideline for tumor imaging with ^{18}F-FDG PET/CT. J Nucl Med 47:885–895
34. Lee SM, Kim TS, Lee JW, Kim SK, Park SJ, Han SS (2011) Improved prognostic value of standardized uptake value corrected for blood glucose level in pancreatic cancer using F-^{18}FDG PET. Clin Nucl Med 36:331–336
35. Nozawa A, Rivandi AH, Kesari S, Hoh CK (2013) Glucose corrected standardized uptake value (SUV_{gluc}) in the evaluation of brain lesions with ^{18}F-FDG PET. Eur J Nucl Med Mol Imaging 40:997–1004
36. Decarie PO, Lepanto L, Billiard JS, Olivie D, Murphy-Lavallee J, Kauffmann C et al (2011) Fatty liver deposition and sparing: a pictorial review. Insights Imaging 2:533–538
37. Sugawara Y, Zasadny KR, Neuhoff AW, Wahl RL (1999) Reevaluation of the standardized uptake value for FDG: variations with body weight and methods for correction. Radiology 213:521–525